Nonreciprocal Amplification with Four-Level Hot Atoms

Gongwei Lin,[1] Shicheng Zhang,[1,2] Yiqi Hu,[1,2] Yueping Niu,[1,3,*] Jiangbin Gong,[4,†] and Shangqing Gong[1,3,‡]
[1]Department of Physics, East China University of Science and Technology, Shanghai 200237, China
[2]School of Materials Science and Engineering, East China University of Science and Technology, Shanghai 200237, China
[3]Shanghai Engineering Research Center of Hierarchical Nanomaterials, Shanghai 200237, China
[4]Department of Physics, National University of Singapore, 117542 Singapore

(Received 20 November 2018; published 18 July 2019)

Optical nonreciprocity is of paramount importance to optical signal processing and one-way optical communication. Here, we theoretically and experimentally demonstrate nonreciprocal amplification based on four-level hot atoms by exploiting atomic Doppler shifts. Our approach is simple and easy to implement. In fair agreement with our theoretical modeling, forward power amplification of 26 dB and backward isolation of 30 dB are observed. Our results will open up a new avenue towards realistic devices based on nonreciprocal amplification.

DOI: 10.1103/PhysRevLett.123.033902

As a symmetry-breaking effect, optical nonreciprocity is of vast interest to science and engineering [1–4]. The conventional route to optical nonreciprocity, which is based on the magneto-optical Faraday effect, always needs bulky magnets and is thus incompatible with integrated circuit technology [5]. During recent years, researchers across different communities have turned to other physical effects to realize magnet-free optical nonreciprocity, including the use of nonlinear optics [6–9], spatiotemporal modulation of permittivity [2,10,11], optomechanical interaction [12–18], interfering parametric processes [19–21], "moving" Bragg mirror [22], cold atomic Bragg lattice [23], chiral quantum optics [24–26], complex optical potentials [27], and thermal motion of hot atoms [28].

Nonreciprocal amplification is essential in communication and signal processing, offering a means to protect the signal source from extraneous noise. Theoretical proposals to realize nonreciprocal amplification have covered Josephson circuits [29,30], reservoir engineering [31], non-Hermitian systems [32], and optomechanical systems [33]. Nonetheless, only scattered experimental realizations of nonreciprocal amplification have been reported, including microwaves in superconductor circuits [34,35] and optical waves in cavity optomechanical systems [36,37].

In this Letter, we put forward a theoretical model based on four-level atoms and accordingly realize nonreciprocal amplification using hot rubidium (Rb) atoms. The mechanism in our innovative approach is an interplay of the Doppler shifts associated with hot atoms, the resultant directional electromagnetically induced transparency (EIT) due to a symmetry-breaking control laser, and a pump laser that induces amplified transmission along the EIT direction only. Experimentally, forward power amplification up to 26 dB and backward power suppression of 30 dB are observed. Compared with the existing experimental realizations of nonreciprocal optical amplification, our scheme is conceptually different and cavity-free, and its realization can be more straightforward.

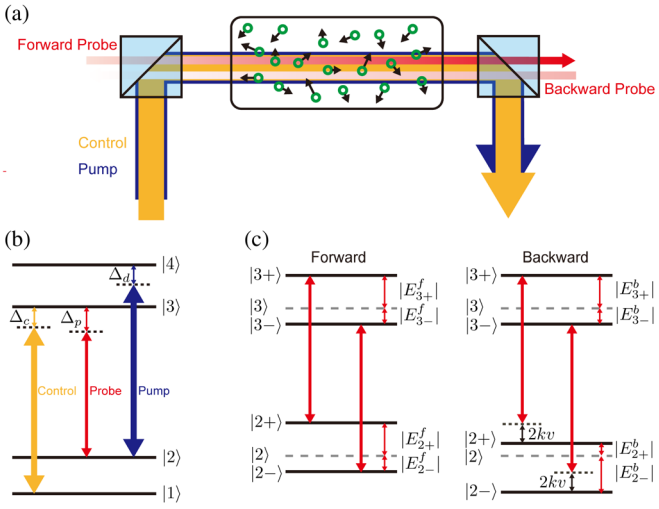

FIG. 1. (a) Schematic of nonreciprocal amplification via atomic Doppler shifts. A control field and a copropagating pump field drive an atomic medium. The forward probe laser goes through the medium with amplification whereas the backward probe laser tuned at the same transition is absorbed by the medium. (b) The level structure of four-level atoms with two lower states $|1\rangle$ and $|2\rangle$ and two higher states $|3\rangle$ and $|4\rangle$. The control field drives the transition $|1\rangle \leftrightarrow |3\rangle$, the pump field drives the transition $|2\rangle \leftrightarrow |4\rangle$, and the probe field is near resonance with the transition $|2\rangle \leftrightarrow |3\rangle$. (c) Dressed states with Doppler shifts accounted for, for forward and backward probe fields, respectively. For two near-resonance gain transition channels $|3+\rangle \leftrightarrow |2+\rangle$ and $|3-\rangle \leftrightarrow |2-\rangle$, they are almost Doppler-free in the case of forward propagation but still significantly Doppler broadened in the case of backward propagation.

The schematic of our approach to nonreciprocal amplification is depicted in Fig. 1(a). There the hot Rb atoms in the cell are driven by a control laser and a pump laser in the same direction. The atomic level structure is modeled by four levels in Fig. 1(b), along with the control field and the pump field driving their respective atomic transitions $|1\rangle \leftrightarrow |3\rangle$ and $|2\rangle \leftrightarrow |4\rangle$. The Rabi frequencies (carrier frequencies) of the control, pump, and probe fields are, respectively, denoted by Ω_c (ω_c), Ω_d (ω_d), and Ω_p (ω_p). The spontaneous decay rates of state $|3\rangle$ ($|4\rangle$) to states $|1\rangle$ and $|2\rangle$ are Γ_{31} (Γ_{41}) and Γ_{32} (Γ_{42}), respectively. The dephasing rate between $|1\rangle$ and $|2\rangle$ is Γ_{21}. Because of the pump field, the atomic populations starting from $|2\rangle$ will experience a transfer pathway $|2\rangle \rightarrow |4\rangle \rightarrow |1\rangle \rightarrow |3\rangle \rightarrow |2\rangle$, through which the probe field can be amplified [38]. In the presence of atomic thermal motion (to be elaborated below), the forward probe field can still be greatly amplified because in our laser-atom configuration the Doppler shifts are canceled with respect to two-photon detuning [39], whereas the backward probe field can be almost completely absorbed because enhanced Doppler effects tune the system far away from two-photon resonance.

Before presenting theoretical results, we first adopt the rather standard dressed-state picture to better digest our motivation and the physical mechanism. To that end, one starts with the interaction Hamiltonian describing the four-level atoms driven by the control and the pump fields in the rotating-wave approximation, $H_{\rm in}=\hbar(\Delta_c-\Delta_p)\sigma_{22}+\hbar\Delta_c\sigma_{33}+\hbar(\Delta_c-\Delta_p+\Delta_d)\sigma_{44}-(\hbar/2)(\Omega_c\sigma_{13}+\Omega_d\sigma_{24}+\text{H.c.})$. Here, $\Delta_p=\omega_p-(\omega_3-\omega_2)$, $\Delta_c=\omega_c-(\omega_3-\omega_1)$, and $\Delta_d=\omega_d-(\omega_4-\omega_2)$ are the respective detunings of the probe, control, and pump fields, $\hbar\omega_i(i=1,2,3,4)$ are the eigenvalues of state $|i\rangle$, and $\sigma_{mn}=|m\rangle\langle n|(m,n=1,2,3,4)$ represent the atomic transition operators. Note, however, that this Hamiltonian is only true in the absence of the Dopper shifts due to the thermal motion of the atoms. Taking into account the longitudinal motion of atoms at randomly distributed velocity v (necessary for hot atoms under consideration here), the frequency detunings of the probe, control, and pump fields are shifted to $\Delta_p \pm k_p v$ (+ for forward propagation and − for backward propagation), $\Delta_c + k_c v$, and $\Delta_d + k_d v$, where k_p, k_c, and k_d are their respective wave vectors. The associated dressed states can then be obtained upon taking into account such Doppler shifts. To simplify the picture one may focus on the situation where $\Delta_c=\Delta_p=\Delta_d=0$, $k_p=k_c=k_d=k$, yielding the following dressed states [39,40],

$$
\begin{aligned}
|3\pm\rangle &= \frac{\lambda_{3\pm}}{\sqrt{\lambda_{3\pm}^2+\Omega_c^2}}|1\rangle + \frac{\Omega_c}{\sqrt{\lambda_{3\pm}^2+\Omega_c^2}}|3\rangle,\\
|2\pm\rangle &= \frac{\lambda_{2\pm}}{\sqrt{\lambda_{2\pm}^2+\Omega_d^2}}|2\rangle + \frac{\Omega_d}{\sqrt{\lambda_{2\pm}^2+\Omega_d^2}}|4\rangle,
\end{aligned}
\tag{1}
$$

with $\lambda_{3\pm}=kv\pm\sqrt{(kv)^2+\Omega_c^2}$ and $\lambda_{2\pm}=kv\pm\sqrt{(kv)^2+\Omega_d^2}$, valid for both forward and backward cases, with, nevertheless, different eigenvalues. For the forward case, the eigenvalues of $|3\pm\rangle$ and $|2\pm\rangle$ are $E_{3\pm}^f=(\hbar/2)\lambda_{3\pm}$ and $E_{2\pm}^f=(\hbar/2)\lambda_{2\pm}$. By contrast, the eigenvalues for the backward case are $E_{3\pm}^b=(\hbar/2)\lambda_{3\pm}$ and $E_{2\pm}^b=(\hbar/2)(\lambda_{2\pm}+4kv)$.

The Doppler shifts are seen from above to have distinct influences on the energy eigenvalues of the dressed states. Figure 1(c) depicts the states dressed by photons, in which there are four possible gain transition channels $|3\pm\rangle \leftrightarrow |2\pm\rangle$. However, the transition channels $|3+\rangle \leftrightarrow |2-\rangle$ and $|3-\rangle \leftrightarrow |2+\rangle$ are far off resonance and can thus be ignored. The probe field in the forward direction would afford two near-resonance transition channels $|3+\rangle \leftrightarrow |2+\rangle$ and $|3-\rangle \leftrightarrow |2-\rangle$ due to a cancellation of the Doppler shifts. The probe field thus has a significant gain. Furthermore, because the probe field does satisfy the two-photon resonance condition with the control field, it exhibits EIT [41,42], and so the gain will accumulate with propagation. By contrast, the two gain channels for a probe field in the backward direction would behave drastically different: They are now fully Doppler broadened and are hence detuned by around $2kv$. Thus, only few atoms with low velocities can contribute to the gain. In addition, the two-photon resonance condition between the probe and the control laser is now also broken by the Doppler shifts, yielding strong absorption by the medium. An amplification of the probe field propagating forward but strong suppression of the same probe field propagating backward thus becomes possible.

Armed with this understanding, we next present numerical results obtained from our theoretical model. The amplification coefficients can be found by solving the steady-state solution of the Liouville equation $(\partial\sigma/\partial t)=-(i/\hbar)[H,\sigma]-\frac{1}{2}\{\Gamma,\sigma\}$, with $H=H_{\rm in}-(\hbar/2)(\Omega_p\sigma_{23}+\text{H.c.})$ being the Hamiltonian including the probe field. The amplification coefficients for forward and backward propagation of the probe field α_f and α_b are defined as $-k_p\text{Im}[\chi_{32}]$, where $\text{Im}[\chi_{32}]$ denotes the imaginary part of the optical susceptibility,

$$
\begin{aligned}
\chi_{32} &= \int_{-\infty}^{+\infty} N(v)\chi_{32}(v)dv\\
&= \int_{-\infty}^{+\infty} \frac{N(v)|u_p|^2}{\epsilon_0\hbar}\frac{\sigma_{32}(v)}{\Omega_p}dv,
\end{aligned}
\tag{2}
$$

with $N(v)=Ne^{-v^2/v_p^2}/(v_p\sqrt{\pi})$ being the Maxwell-Boltzmann velocity distribution, v_p the most probable velocity, N the atomic density, and u_p the transition dipole moment between states $|2\rangle$ and $|3\rangle$. A positive (negative) amplification coefficient indicates amplification

(absorption). Theoretical findings of nonreciprocal transmission are summarized in Fig. 2. In our numerical calculations, we have incorporated the collision broadening effect caused by atomic thermal motion [43]. For atoms at around room temperature, we assume that the broadening effect is proportional to the atomic density, with the associated broadening coefficient set at $\beta = 0.6 \times 10^{-18}$ m^3 according to our experimental conditions. From the shown results of α_f and α_b at $\Delta_p = 0$ vs the pump field strength and control field strength, it is seen that the forward probe field can be nearly transparent or even greatly amplified whereas the backward probe field can be absorbed over a wide parameter regime. In particular, under the condition of $\Omega_d \approx \Omega_c$, the forward case can exhibit enormous amplification and the backward case suffers strong absorption. As a side note, theoretical results also indicate that in the regime of small Ω_c, the peak amplification coefficient α_f (obtained by optimizing Ω_d) increases with Ω_c. However, this trend does not persist for sufficiently large Ω_c. That is, the peak amplification coefficient α_f may decrease with Ω_c [see inset in Fig. 2(a)]. This theoretical observation echoes with a previous result in Ref. [39] and is also consistent with the intuition that the actual amplification performance does have an upper bound. Turning to the backward case, $|\alpha_b|$ gradually decreases as Ω_d increases. For $\Omega_d \gg \Omega_c$, the atomic populations are almost exclusively in the state $|1\rangle$ and the system would become transparent again.

We performed the experiment with hot ^{87}Rb atoms in a vapor cell of 7.5 cm in length. A narrow linewidth tunable laser with wavelength of 795 nm serves as the control field and is tuned to the $D1$ line $5S_{1/2}, F_g = 1(|1\rangle) \rightarrow 5P_{1/2}$, $F_e = 2(|3\rangle)$ transition. Another narrow linewidth tunable laser with wavelength of 780 nm serves as the pump field and is tuned to the $D2$ line $5S_{1/2}$, $F_g = 2(|2\rangle) \rightarrow 5P_{3/2}$, $F_e = 1(|4\rangle)$ transition. A third narrow linewidth tunable laser with wavelength of 795 nm serves as probe field and is tuned to the $D1$ line $5S_{1/2}, F_g = 2(|2\rangle) \rightarrow 5P_{1/2}, F_e = 2(|3\rangle)$ transition. The Rb cell is heated to 65 °C–85 °C in our experiment. The polarization of control and pumping fields is orthogonal to the probe field and misaligned by a small angle to improve the signal-to-noise ratio of the probe field. The radii of the control, pump, and probe fields are estimated to be 800, 800, and 250 μm, respectively. The probe field power is measured by a photoelectric detector. In our experimental system, the four-wave-mixing signal is negligible due to a weak probe field, limited optical length,

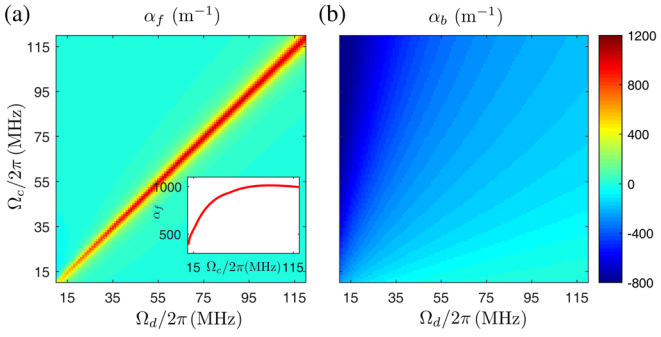

FIG. 2. Theoretical nonreciprocal amplification coefficients α_f and α_b versus the strength of the control and pump fields for forward (a) and backward (b) propagation of the probe field. Parameters: The detunings are $\Delta_p = \Delta_c = \Delta_d = 0$. To better reflect our experimental system and better fit our experimental results, the spontaneous decay rate and dephasing rate of the concerned atomic transitions are modeled by $\{\Gamma_{31}, \Gamma_{32}, \Gamma_{41}, \Gamma_{42}, \Gamma_{21}\} = 2\pi \times \{4.2 + \beta N, 4.2 + \beta N, 5.6 + \beta N, 2.8 + \beta N, 0.1 + \beta N\}$MHz, where $N = 2 \times 10^{18}/\text{m}^3$ and the broadening coefficient is assumed to be $\beta = 0.6 \times 10^{-18}$ m^3. The transition dipole moment for the probe field is $u_p = 1.4 \times 10^{-29}$ C m. The wave vector of the probe field is given by $k_p = 2\pi/\lambda_p$, with $\lambda_p = 795$ nm.

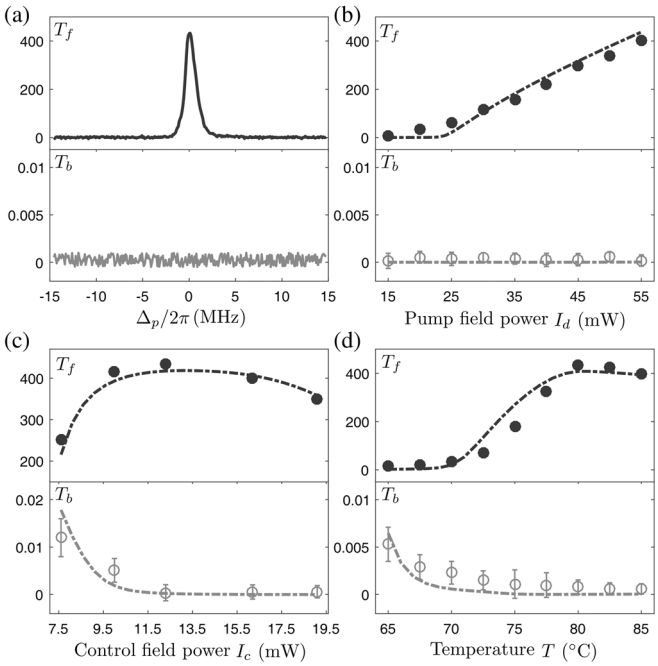

FIG. 3. (a) Experimental observation of normalized forward and backward transmission versus the detuning of the probe field, with pump field power $I_d = 55.0$ mW, control field power $I_c = 16.0$ mW, and temperature $T = 80$ °C. (b) The normalized on-resonance transmission of the probe field versus pump field power at temperature 80 °C, with the control field power fixed at 16.0 mW. (c) The normalized on-resonance transmission versus the control field power at temperature 80 °C, with the pump field power fixed at 55.0 mW. (d) The normalized on-resonance transmission versus temperature, with pump field power fixed at 55.0 mW and control field power fixed at 12.0 mW. In (b)–(d) the dots are experimental results and the dashed lines represent theoretical fittings. Theoretical results are obtained with transition dipole moment $\{u_p, u_c, u_d\} = \{1.4, 1.4, 0.5\} \times 10^{-29}$ C m and effective medium length $L_{\text{eff}} = 5$ cm, and other parameters chosen the same as those in Fig. 2. The probe field power is kept at $I_p = 0.1$ μW for (a)–(d).

and poor phase matching conditions. Before measuring the transmission of the probe field, we also measure the signal without the probe field, confirming that there is no signal along the forward or backward direction except noise. We fix the probe field power at 0.1 μW, corresponding to the Rabi frequency $\Omega_p = 2\pi \times 0.5$ MHz.

Figure 3(a) presents the typical nonreciprocal transmission spectrum of the probe field versus its detuning. The transmission is defined by the output voltage ratio between the detectors associated with the transmitted and input probe fields. We denote the transmission for forward and backward cases by T_f and T_b, respectively. There is a sharp gain peak for the forward case and rather uniform and significant absorption for the backward case. This clearly demonstrates nonreciprocal amplification under near-resonance conditions. The transmission ratio between the forward and backward cases is seen to go well beyond the order of 10^5. For the on-resonance case as an example, Fig. 3(b) depicts our transmission measurement results with a varying pump field power, with the experimental system maintained at 80 °C and the control field power fixed at 16.0 mW ($\Omega_c = 2\pi \times 60$ MHz). It is seen from Fig. 3(b) that as the pump field power increases from 15.0 to 55.0 mW (Ω_d increases from $2\pi \times 21$ MHz to $2\pi \times 41$ MHz, the highest power we can achieve in our setup), the forward transmission increases from 8.7 to 400.5, whereas the backward transmission is observed to stay at a very low level (note also the electrical noise in our readings).

To further investigate the best experimental parameters for nonreciprocal amplification, we have also scanned the control field power from 7.6 to 19.1 mW under a pump field power fixed at 55.0 mW. The measured transmission results are shown in Fig. 3(c). The highest forward transmission of 433.5 is seen to occur for a control field power at 12.0 mW, with the associated Rabi frequency $\Omega_c = 2\pi \times 52$ MHz, slightly larger than $\Omega_d = 2\pi \times 41$ MHz. This is interesting because the energy eigenvalues $E^f_{3\pm}$ and $E^f_{2\pm}$ of the dressed states would suggest that optimal amplification occurs at $\Omega_c = \Omega_d$. To better understand this observation, we have also carried out theoretical simulations to include the propagation effects. For these three fields, their propagation can be described by $\partial\Omega_n(z)/\partial z = -k_n \mathrm{Im}[\chi_{ij}(z)]$ (n stands for c, p, or d). In this regard, it is necessary to note that in our system the transition dipole moment of the control field is larger than that of the pump field, and that the rate of spontaneous emission from state $|4\rangle$ to state $|1\rangle$ is larger than that from state $|4\rangle$ to state $|2\rangle$. As shown in Fig. 4, the absorption of the control field becomes stronger than that of the pump field due to propagation, thus indeed requiring that the input control field power be slightly larger than that of the pump field to yield an optimal amplification.

We have also measured temperature effects on nonreciprocal amplification. The transmission versus temperature with all field strengths fixed at a particular set of values is presented in Fig. 3(d). It is observed that as the temperature increases from 65 °C to 85 °C, the forward transmission first increases rapidly but then drops slightly when the temperature is beyond 80 °C. To understand this result, we note that an increase in temperature results in an increase of the atomic density of our medium (from $4.9 \times 10^{17}/\mathrm{m}^3$ to $2.2 \times 10^{18}/\mathrm{m}^3$), which is equivalent to an increase in the optical propagation length. Referring again to Fig. 4, the effective pump field strength in the medium can become much larger than that of the control field when the propagation length is sufficiently large. This then leads to atomic populations almost exclusively in the state $|1\rangle$, thus yielding saturation in the amplification. Moreover, a higher atomic density due to the increase in temperature leads to more frequent collisions and hence more severe decoherence, thereby causing amplification to degrade.

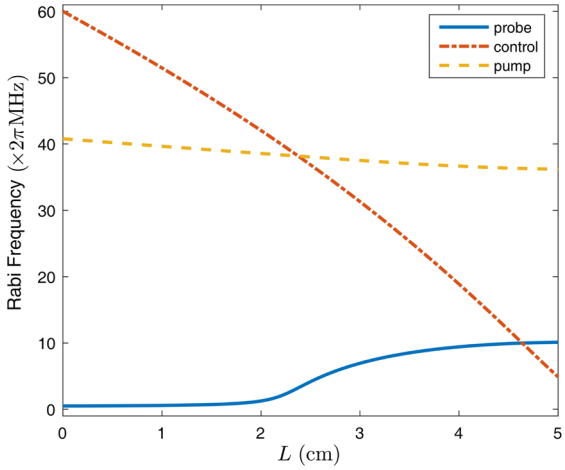

FIG. 4. Rabi frequencies of three laser fields versus propagation length. The input Rabi frequencies of the probe, control, and pump fields are $2\pi \times 0.5$ MHz, $2\pi \times 60$ MHz, and $2\pi \times 41$ MHz, respectively. Other parameters are the same as in Fig. 2.

Considering all the observations made above and given the current constraints in our experimental platform, the best we have experimentally achieved is a forward amplification of 26 dB [i.e., $10\log(T_f)$] together with a backward suppression of 30 dB [i.e., $-10\log(T_b)$] (calculated from an averaged backward transmission). Furthermore, all our experimental results are found to be well fitted by our theoretical model [see dashed lines in Figs. 3(b)–3(d)] using one reasonable set of system parameters and including broadening effects that are assumed to be proportional to the atomic density of the medium. We also comment on the performance of our system near the quantum noise limit, where the main noise comes from the spontaneous emission [44]. Following the standard Heisenberg-Langevin approach [45], we theoretically obtained the spontaneous emission noise amplification factor using our experimental parameters. It is found that the obtained noise amplification factor is larger than the signal

amplification factor under near-resonance conditions. Thus our system may have limitations when amplifying very weak quantum optical signals.

In summary, we have presented here both theory and a straightforward experimental realization of nonreciprocal amplification using four-level hot atoms. Our approach is motivated by clear physical insights, and it is robust and easy to implement. We have demonstrated magnet-free optical nonreciprocity, with 26 dB forward amplification and 30 dB backward isolation. Different from previous experiments for nonreciprocal amplification of optical wave with a cavity optomechanical system [36,37], our realization exploited hot atoms and there is no need for a high-Q factor cavity. We are also optimistic about the potential of our approach towards miniaturization and integration, considering that the length of the Rb cell can be reduced to nanometers without losing important quantum coherence effect [46] and that hot atoms may be trapped in one-dimensional waveguides [47].

This work was supported by the National Natural Science Foundation of China (Grants No. 11774089, No. 11674094, and No. 11474092) and Shanghai Natural Science Foundation (Grants No. 18DZ2252400, No. 17ZR1442700, and No. 18ZR1410500).

G. W. L. and S. C. Z. contributed equally to this work.

*niuyp@ecust.edu.cn
†phygj@nus.edu.sg
‡sqgong@ecust.edu.cn

[1] A. B. Khanikaev and A. Alù, Nat. Photonics **9**, 359 (2015).
[2] Z. Yu and S. Fan, Nat. Photonics **3**, 91 (2009).
[3] P. Lodahl, S. Mahmoodian, S. Stobbe, A. Rauschenbeutel, P. Schneeweiss, J. Volz, H. Pichler, and P. Zoller, Nature (London) **541**, 473 (2017).
[4] J. I. Cirac, P. Zoller, H. J. Kimble, and H. Mabuchi, Phys. Rev. Lett. **78**, 3221 (1997).
[5] L. Bi, J. Hu, P. Jiang, D. H. Kim, G. F. Dionne, L. C. Kimerling, and C. A. Ross, Nat. Photonics **5**, 758 (2011).
[6] N. Bender, S. Factor, J. D. Bodyfelt, H. Ramezani, D. N. Christodoulides, F. M. Ellis, and T. Kottos, Phys. Rev. Lett. **110**, 234101 (2013).
[7] L. Fan, J. Wang, L. T. Varghese, H. Shen, B. Niu, Y. Xuan, A. M. Weiner, and M. Qi, Science **335**, 447 (2012).
[8] L. Chang, X. Jiang, S. Hua, C. Yang, J. Wen, L. Jiang, G. Li, G. Wang, and M. Xiao, Nat. Photonics **8**, 524 (2014).
[9] B. Peng, Ş. K. Özdemir, F. Lei, F. Monifi, M. Gianfreda, G. L. Long, S. Fan, F. Nori, C. M. Bender, and L. Yang, Nat. Phys. **10**, 394 (2014).
[10] N. A. Estep, D. L. Sounas, J. Soric, and A. Alù, Nat. Phys. **10**, 923 (2014).
[11] M. S. Kang, A. Butsch, and P. St. J. Russell, Nat. Photonics **5**, 549 (2011).
[12] F. Ruesink, J. P. Mathew, M.-A. Miri, and E. Verhagen, Nat. Commun. **9**, 1798 (2018).
[13] M. Hafezi and P. Rabl, Opt. Express **20**, 7672 (2012).
[14] Z. Shen, Y.-L. Zhang, Y. Chen, C.-L. Zou, Y.-F. Xiao, X.-B. Zou, F.-W. Sun, G.-C. Guo, and C.-H. Dong, Nat. Photonics **10**, 657 (2016).
[15] F. Ruesink, M.-A. Miri, A. Alù, and E. Verhagen, Nat. Commun. **7**, 13662 (2016).
[16] G. A. Peterson, F. Lecocq, K. Cicak, R. W. Simmonds, J. Aumentado, and J. D. Teufel, Phys. Rev. X **7**, 031001 (2017).
[17] S. Barzanjeh, M. Wulf, M. Peruzzo, M. Kalaee, P. B. Dieterle, O. Painter, and J. M. Fink, Nat. Commun. **8**, 953 (2017).
[18] N. R. Bernier, L. D. Tóth, A. Koottandavida, M. A. Ioannou, D. Malz, A. Nunnenkamp, A. K. Feofanov, and T. J. Kippenberg, Nat. Commun. **8**, 604 (2017).
[19] A. Kamal, J. Clarke, and M. H. Devoret, Nat. Phys. **7**, 311 (2011).
[20] A. Kamal, A. Roy, J. Clarke, and M. H. Devoret, Phys. Rev. Lett. **113**, 247003 (2014).
[21] S. Hua, J. Wen, X. Jiang, Q. Hua, L. Jiang, and M. Xiao, Nat. Commun. **7**, 13657 (2016).
[22] S. A. R. Horsley, J.-H. Wu, M. Artoni, and G. C. La Rocca, Phys. Rev. Lett. **110**, 223602 (2013).
[23] D.-W. Wang, H.-T. Zhou, M.-J. Guo, J.-X. Zhang, J. Evers, and S.-Y. Zhu, Phys. Rev. Lett. **110**, 093901 (2013).
[24] C. Sayrin, C. Junge, R. Mitsch, B. Albrecht, D. O'Shea, P. Schneeweiss, J. Volz, and A. Rauschenbeutel, Phys. Rev. X **5**, 041036 (2015).
[25] M. Scheucher, A. Hilico, E. Will, J. Volz, and A. Rauschenbeutel, Science **354**, 1577 (2016).
[26] K. Xia, G. Lu, G. Lin, Y. Cheng, Y. Niu, S. Gong, and J. Twamley, Phys. Rev. A **90**, 043802 (2014).
[27] L. Feng, M. Ayache, J. Huang, Y.-L. Xu, M.-H. Lu, Y.-F. Chen, Y. Fainman, and A. Scherer, Science **333**, 729 (2011).
[28] S. Zhang, Y. Hu, G. Lin, Y. Niu, K. Xia, J. Gong, and S. Gong, Nat. Photonics **12**, 744 (2018).
[29] B. Abdo, K. Sliwa, S. Shankar, M. Hatridge, L. Frunzio, R. Schoelkopf, and M. Devoret, Phys. Rev. Lett. **112**, 167701 (2014).
[30] B. Abdo, K. Sliwa, L. Frunzio, and M. Devoret, Phys. Rev. X **3**, 031001 (2013).
[31] A. Metelmann and A. A. Clerk, Phys. Rev. X **5**, 021025 (2015).
[32] T. T. Koutserimpas and R. Fleury, Phys. Rev. Lett. **120**, 087401 (2018).
[33] D. Malz, L. D. Tóth, N. R. Bernier, A. K. Feofanov, T. J. Kippenberg, and A. Nunnenkamp, Phys. Rev. Lett. **120**, 023601 (2018).
[34] K. M. Sliwa, M. Hatridge, A. Narla, S. Shankar, L. Frunzio, R. J. Schoelkopf, and M. H. Devoret, Phys. Rev. X **5**, 041020 (2015).
[35] F. Lecocq, L. Ranzani, G. A. Peterson, K. Cicak, R. W. Simmonds, J. D. Teufel, and J. Aumentado, Phys. Rev. Applied **7**, 024028 (2017).
[36] K. Fang, J. Luo, A. Metelmann, M. H. Matheny, F. Marquardt, A. A. Clerk, and O. Painter, Nat. Phys. **13**, 465 (2017).
[37] Z. Shen, Y.-L. Zhang, Y. Chen, F.-W. Sun, X.-B. Zou, G.-C. Guo, C.-L. Zou, and C.-H. Dong, Nat. Commun. **9**, 1797 (2018).

[38] H. Kang, L. Wen, and Y. Zhu, Phys. Rev. A **68**, 063806 (2003).
[39] L. B. Kong, X. H. Tu, J. Wang, Y. Zhu, and M. S. Zhan, Opt. Commun. **269**, 362 (2007).
[40] C. Y. Ye, A. S. Zibrov, Yu. V. Rostovtsev, and M. O. Scully, Phys. Rev. A **65**, 043805 (2002).
[41] K.-J. Boller, A. Imamoğlu, and S. E. Harris, Phys. Rev. Lett. **66**, 2593 (1991).
[42] M. Fleischhauer, A. Imamoğlu, and J. P. Marangos, Rev. Mod. Phys. **77**, 633 (2005).
[43] W. Demtröder, *Laser Spectroscopy* (Springer, Kaiserslautern, 2008).
[44] P. R. Battle, R. C. Swanson, and J. L. Carlsten, Phys. Rev. A **44**, 1922 (1991).
[45] C. Cohen-Tannoudji, J. Dupon-Roc, and G. Grynberg, *Atom-Photon Interaction* (Wiley, New York, 1992).
[46] J. Keaveney, A. Sargsyan, U. Krohn, I. G. Hughes, D. Sarkisyan, and C. S. Adams, Phys. Rev. Lett. **108**, 173601 (2012).
[47] M. R. Sprague, P. S. Michelberger, T. F. M. Champion, D. G. England, J. Nunn, X.-M. Jin, W. S. Kolthammer, A. Abdolvand, P. St. J. Russell, and I. A. Walmsley, Nat. Photonics **8**, 287 (2014).